Article

Current Biology

In vitro experiments and kinetic models of *Arabidopsis* pollen hydration mechanics show that MSL8 is not a simple tension-gated osmoregulator

Graphical abstract

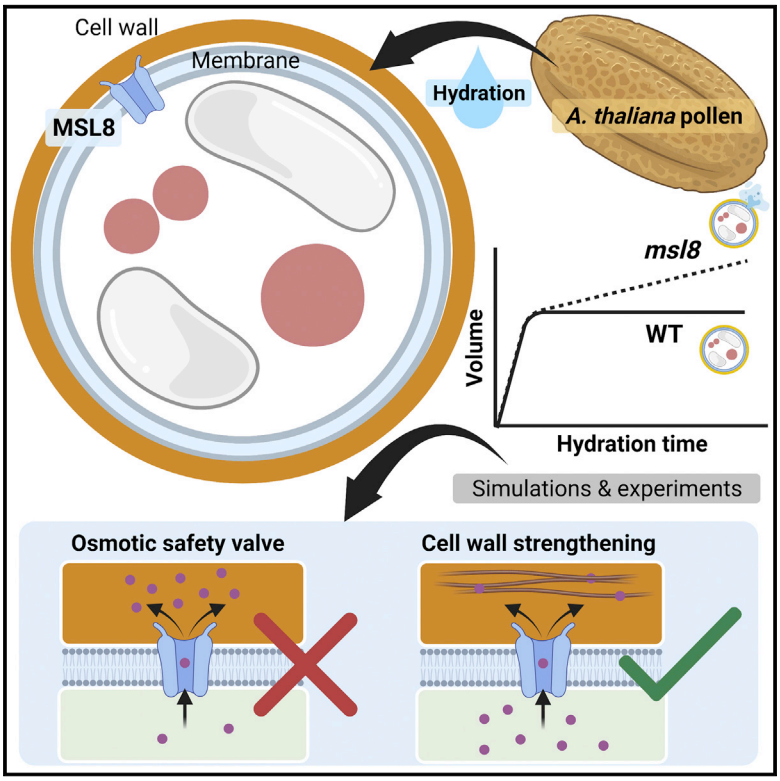

Highlights

- Pollen lacking mechanosensitive channel MSL8 does not stabilize volume after hydration
- A model for MSL8 as a tension-gated osmoregulator does not replicate pollen behavior
- Multiple perturbations were tested both experimentally and computationally
- A model wherein MSL8 strengthens the cell wall best fits the experimental responses

Authors

Kari Miller, Wanda Strychalski, Masoud Nickaeen, Anders Carlsson, Elizabeth S. Haswell

Correspondence

ehaswell@wustl.edu

In brief

Miller et al. use complementary mathematical modeling and laboratory experiments to show that the mechanosensitive ion channel MscS-like 8 does not act as a simple osmotic safety valve. Instead, MSL8 may strengthen the cell wall, allowing volume stabilization and survival during hydration on the stigma.

Miller et al., 2022, Current Biology *32*, 1–14
July 11, 2022
https://doi.org/10.1016/j.cub.2022.05.033

CellPress

Current Biology

CellPress

Article

In vitro experiments and kinetic models of *Arabidopsis* pollen hydration mechanics show that MSL8 is not a simple tension-gated osmoregulator

Kari Miller,[1,2] Wanda Strychalski,[3] Masoud Nickaeen,[4,6] Anders Carlsson,[2,5] and Elizabeth S. Haswell[1,2,7,8,*]
[1]Department of Biology, Washington University, St. Louis, MO 63130, USA
[2]NSF Center for Engineering Mechanobiology, Cleveland, OH, USA
[3]Department of Mathematics, Applied Mathematics, and Statistics, Case Western Reserve University, Cleveland, OH 44106, USA
[4]University of Connecticut School of Medicine, Farmington, CT 06030, USA
[5]Department of Physics, Washington University, St. Louis, MO 63130, USA
[6]Present address: Metrum Research Group, Tariffville, CT 06081, USA
[7]Twitter: @ehaswell
[8]Lead contact
*Correspondence: ehaswell@wustl.edu
https://doi.org/10.1016/j.cub.2022.05.033

SUMMARY

Pollen, a neighbor-less cell containing the male gametes, undergoes mechanical challenges during plant sexual reproduction, including desiccation and rehydration. It was previously shown that the pollen-specific mechanosensitive ion channel MscS-like (MSL)8 is essential for pollen survival during hydration and proposed that it functions as a tension-gated osmoregulator. Here, we test this hypothesis with a combination of mathematical modeling and laboratory experiments. Time-lapse imaging revealed that wild-type pollen grains swell, and then they stabilize in volume rapidly during hydration. *msl8* mutant pollen grains, however, continue to expand and eventually burst. We found that a mathematical model, wherein MSL8 acts as a simple-tension-gated osmoregulator, does not replicate this behavior. A better fit was obtained from variations of the model, wherein MSL8 inactivates independent of its membrane tension gating threshold or MSL8 strengthens the cell wall without osmotic regulation. Experimental and computational testing of several perturbations, including hydration in an osmolyte-rich solution, hyper-desiccation of the grains, and MSL8-YFP overexpression, indicated that the cell wall strengthening model best simulated experimental responses. Finally, the expression of a nonconducting MSL8 variant did not complement the *msl8* overexpansion phenotype. These data indicate that contrary to our hypothesis and to the current understanding of MS ion channel function in bacteria, MSL8 does not act as a simple membrane tension-gated osmoregulator. Instead, they support a model wherein ion flux through MSL8 is required to alter pollen cell wall properties. These results demonstrate the utility of pollen as a cellular scale model system and illustrate how mathematical models can correct intuitive hypotheses.

INTRODUCTION

Plant cells are unique mechanical systems. They have a strong, yet flexible, outer wall containing a soft, but turgid, protoplast and are often physically connected to their neighbors.[1] Their turgor pressure must be controlled during growth, development, and osmotic changes to maintain cell and tissue integrity and to mediate cell and tissue movements.[2,3] Although our understanding of plant cell mechanics has contributed to mechanical models of plant tissue development,[4] wall-to-wall adhesion adds external forces and responses that complicate the mechanical characterization of any one cell.[5] Here, we employ pollen grains as a neighbor-less model system for the biomechanical characterization of plant cells.

Pollen grains, which are the male gametophyte, undergo drastic mechanical changes throughout their normal development. After meiosis and one or two rounds of mitosis, each grain desiccates within the anther to slow metabolism and protect itself from environmental conditions.[6] Pollen from some species, including the model flowering plant *Arabidopsis thaliana*, eventually contain less than 30% water.[6] Dry grains are then released from the anther to travel on pollinators or by air to reach the stigma, the receptive part of the flower. Once a compatible association is formed, pollen grains rehydrate in about 10 min, using moisture from the female tissue.[7] The now metabolically active pollen extends a tube that passes through stigmatic tissue to reach an ovule. Finally, the tube tip bursts and releases the sperm cells for fertilization. The entire process of delivery to the egg requires careful control of pollen cell mechanics to prevent premature lysing while also maintaining rapid growth.[8] A deeper understanding of the mechanics of this process is relevant to agriculture, ecology, and climate change, as all angiosperms require pollen to reproduce and pollen grains are sensitive to high temperature.[6]

Please cite this article in press as: Miller et al., *In vitro* experiments and kinetic models of *Arabidopsis* pollen hydration mechanics show that MSL8 is not a simple tension-gated osmoregulator, Current Biology (2022), https://doi.org/10.1016/j.cub.2022.05.033

Both mechanical and signaling components are known to contribute to pollen hydration. The pollen grain cell wall is mostly covered by a tough and water-insoluble outer layer called the exine. Areas of the wall lacking the exine, called apertures, allow for folding and unfolding of the cell wall and can provide a route for pollen tube emergence and water entry.[9] The exine is covered in a lipid and protein-based layer called the pollen coat, components of which are essential for establishing a productive interaction with the stigma prior to hydration.[10] Pectin in the cell wall may also contribute to pollen hydration dynamics.[11–13] In the plasma membrane, aquaporins are important for water transport during in vivo hydration,[14] and the mechanosensitive (MS) ion channel MscS-like (MSL)8 plays a key role in maintaining pollen grain integrity during hydration and germination.[15–17] Several signaling proteins, such as those related to the SnRK1 complex, are required for pollen hydration on the stigma.[10]

MS channels are known to contribute to cell survival and/or volume regulation during hypoosmotic shock in all kingdoms of life.[5,18–20] This function has been explored in *E. coli* where MS channels of small (MscS) and large (MscL) conductance open in response to elevated membrane tension.[21–23] MscS and MscL are required for *E. coli* to survive and recover from hypoosmotic shock,[24–28] supporting a hypothesis wherein mechanosensitive channels serve as "osmotic safety valves."[29–31] According to this theory, the increase in plasma membrane tension caused by cell swelling opens MscS and MscL channels, leading to the release of osmolytes, reducing turgor pressure, and preventing cellular lysis. In support of this idea, mathematical models of hypoosmotic shock require MscS and MscL channel activity to accurately simulate the observed volume changes of *E. coli* cells.[32]

We have previously proposed that MSL8 performs a similar function in pollen.[15,16] MSL8 localizes to the plasma membrane, and pollen lacking MSL8 shows a dramatically decreased viability compared with wild type (WT) after 2 h of *in vitro* hydration in water.[15] Moreover, when pore-blocking point mutations are introduced into MSL8, or it is not properly localized to the plasma membrane, pollen grains no longer maintain viability during *in vitro* hydration.[16,33] Although these observations support the idea that like bacterial MS ion channels, MSL8 acts as an osmotic safety valve, direct evidence of ion flux through MSL8 during the early stages of hydration is lacking. Given the complex genetic interactions between MSL8 and the cell wall integrity signaling pathway,[17] it is possible that MSL8 contributes to cellular integrity during hydration through signaling rather than through ion flux, or that ion flux through MSL8 has functions other than osmoregulation. Here, we combined experiments and mathematical modeling to test the osmotic safety valve hypothesis for MSL8 function in pollen hydration.

RESULTS

In vitro hydrating pollen grains lacking MSL8 continue to expand for minutes, whereas WT grains stabilize within 30 s

To better understand the mechanics of pollen hydration and test our hypothesis that MSL8 is a tension-gated osmoregulator, we developed an assay to quantify pollen size changes during the initial stages of hydration. Fresh pollen was placed onto a glass bottom dish for imaging, and a recording sequence was started directly before a drop of deionized (DI) water was applied. Most pollen grains stuck to the bottom of the dish, allowing for consistent imaging (Figure 1A). By the end of hydration, WT pollen expanded ~6.5 μm in width but shrank ~1.5 μm in length (Figure 1B). Any pollen that visibly burst was excluded from the analysis.

We took measurements every ~0.5 s over the course of 165 s and used these dimensions to estimate the volume of an approximated 3-dimensional ellipsoid shape lying on the substrate. We then calculated the relative volume change: (initial volume − current volume)/initial volume. This value allowed us to normalize against variation in the initial desiccated grain size between WT and *msl8* mutant pollen (Figures S1A–S1D). WT pollen grains rapidly expanded, and after about 28 s of exposure to DI water, stabilized with a final volume increase of ~60% that did not significantly change after 165 s of exposure (Figures 1C, 1D, and S1E). We repeated this assay with pollen from an *msl8* null mutant, *msl8-5*, that was previously created via CRISPR–Cas9 gene editing.[17] As expected,[15,17] *msl8* mutant pollen had a higher number of bursting events than the WT (12% versus 1.5%; Figure S1F). Although *msl8* pollen grains that remained intact for the duration of the assay initially swelled with the same kinetics as WT pollen, they continued to expand in both length and width throughout the time course, achieving an extra 12% expansion after initial rapid hydration (Figures 1C, 1D, and S1G). We observed this same phenotype in another *msl8* mutant line (*msl8-8*) and two *msl7-1 msl8* mutant lines (*msl7-1 msl8-6* and *msl7-1 msl8-7*)[17] (Figure S1H). MSL7 is closely related to MSL8 but is expressed only in pollen tubes and stigma cells, and there is no known phenotype for *msl7-1* mutants.[17] These results suggested that MSL8 is required to control the buildup of turgor in response to hypoosmotic swelling, which follows our hypothesis that MSL8 acts as an osmotic safety valve.

A simple kinetic model of pollen hypoosmotic swelling fails to reproduce experimental observations

To simulate the experimental data and test our assumptions about the system, we developed an ordinary differential equation that describes pollen grain expansion. This model incorporated several key properties of pollen, including an osmolyte-rich protoplast, a resilient cell wall, and MSL8 channel function. We approximated the pollen grain as a sphere and modeled the outside of the pollen grain as a single unit, with cell wall stiffness resisting internal turgor pressure. The parameter values used are shown in Table 1 and further explained in the STAR Methods. The membrane stiffness was used for calculating membrane tension, but its contribution to cell stiffness was considered negligible. We assumed that the plasma membrane does not renew (see discussion). Most parameter values were estimated using existing measurements in the literature,[15,23,28,34–37] but those that were unavailable were fitted to the data.

Each time step of the simulation began by calculating the membrane tension (σ) based on the stiffness of the membrane and the size of the pollen grain at that point in time:

$$\sigma = K_m\left(\frac{r}{r_0} - 1\right), \qquad \text{(Equation 1)}$$

Please cite this article in press as: Miller et al., *In vitro* experiments and kinetic models of *Arabidopsis* pollen hydration mechanics show that MSL8 is not a simple tension-gated osmoregulator, Current Biology (2022), https://doi.org/10.1016/j.cub.2022.05.033

CellPress

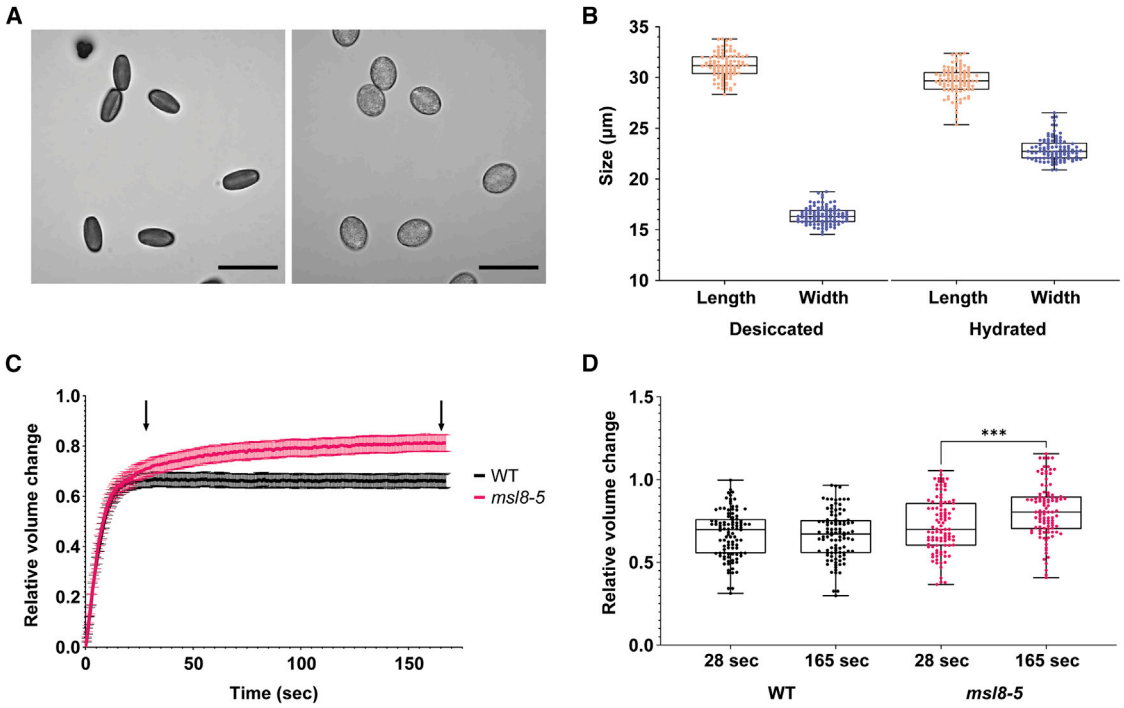

Figure 1. *In vitro* hydrating *msl8* mutant pollen grains continue to expand, while WT grains stabilize within 28 s

(A) Image of *Arabidopsis thaliana* pollen before and after addition of DI water. Scale bars, 50 μm.

(B) Length and width both before and after *in vitro* hydration of WT pollen (n = 100 grains per treatment). Boxes are 1st quartile, median, and 3rd quartile, while whiskers are minimum and maximum values.

(C) Relative pollen grain volume over time (n = 100 grains per genotype). Volume calculated assuming an ellipsoid shape and each pollen grain is normalized to itself. Bars are 95% confidence intervals (CI).

(D) Comparison of the relative volume after the initial rapid hydration (the 28 s time point) and at the end of the assay (165 s). These time points are indicated with arrows in (C). The Mann-Whitney test was used to compare *msl8-5* with itself ($p < 0.005$) and WT with itself ($p = 0.70$).

See also Figure S1.

where K_m is the membrane stiffness, r is the radius, and r_0 is the initial radius. Our initial model assumed that when membrane tension reaches the opening tension (σ_{open}) threshold of MSL8, the channel will begin to release osmolytes. When the membrane tension drops back below the threshold, osmolyte release stops. The rate of change in osmolyte concentration is

$$\frac{dc_0}{dt} = -k_{flux}c_0 \text{ if } \sigma > \sigma_{open}, \quad \text{(Equation 2)}$$

where c_0 is the total number of osmolyte molecules divided by the initial volume and k_{flux} is the rate of ion flux through MSL8. Finally, we calculated the current osmolyte concentration (c):

$$c = c_0\left(r_0/r\right)^3. \quad \text{(Equation 3)}$$

Then, we determined the change in radius (r) as water follows the osmotic gradient and enters the pollen grain:

$$\frac{dr}{dt} = L_p\left[RT(c - c_{ext}) - 2\left(\frac{K}{r}\right)\left(\frac{r}{r_0} - 1\right)\right], \quad \text{(Equation 4)}$$

where L_p is the water permeability, K is the stiffness of the cell wall, c_{ext} is the external osmolyte concentration, R is the Boltzmann constant, and T is temperature. The second term inside the brackets represents the Laplace pressure corresponding to the membrane tension.

We ran two initial simulations: one that included the MSL8 channel function (representing WT pollen) and one that removed channel function such that osmolytes never exit the grain (representing *msl8* pollen) (Figure 2A). This simulation assumed that when the gating tension is reached, all channels open to release osmolytes. We did test the idea that channels open gradually by incorporating a slow increase in the k_{flux} value after σ_{open} is reached, but it did not make any appreciable difference in the results. Thus, we retained the assumption that all channels open at once when σ_{open} is surpassed. We noticed three main discrepancies between the simulations and experimental data or the accepted values from the literature. First, the predicted membrane tension was about four times higher than the estimated membrane lytic tension of a protoplast (10 mN m^{-1}),[38] as shown on the right y axis in Figure 2A. Second, the WT simulation showed volume increasing rapidly, peaking, and then steadily decreasing, whereas experimental data showed WT pollen volume stabilizing after about 30 s. Third, the *msl8* simulation predicted a relatively rapid stabilization of the volume, but experimental data showed continued expansion for at least 150 s.

Please cite this article in press as: Miller et al., *In vitro* experiments and kinetic models of *Arabidopsis* pollen hydration mechanics show that MSL8 is not a simple tension-gated osmoregulator, Current Biology (2022), https://doi.org/10.1016/j.cub.2022.05.033

Table 1. Parameters used in pollen hydration models

Notation	Value used	Definition	Reference
Physical property of the cell			
r_0	1.05×10^{-5} m	Initial cell radius	Direct measurement; Figure 1
K	87.5 N m^{-1}	Stiffness calculated by multiplying the elastic modulus of the cell wall (350 MPa) by the cell wall thickness (0.25 μm)	Nezhad et al.[37] (elastic modulus); Suzuki et al.[36] (wall thickness estimated from TEM image of WT)
K_m	0.230 N m^{-1}	Membrane stiffness	Wolfe and Steponkus[34]
c_0	1.81 OR 1.54 M	Total number of osmolytes divided by the initial cell volume	Fitted to data
c_{ext}	0 M	External osmotic concentration. Assumed to be 0 for water, calculated for 20% PEG.	Property of deionized water; Schiller et al.[35] (PEG)
	0.33 M		
L_p	8.89×10^{-14} m Pa^{-1} s^{-1}[a,b]	Water permeability	Fitted to data
	1.04×10^{-13} m Pa^{-1} s^{-1}[c]		
ε_{min}	0.164[a]	Strain value that induces stress; dimensionless	Fitted to data
	0.150[b]		
	0.126[c]		
MSL8 channel			
σ_{open}	0.005 N m^{-1}	Estimated gating tension of MSL8; make this infinitely large to get the *msl8* simulation	Sukharev[23]
k_{flux}	2.36×10^{-3} s^{-1}	Rate of osmolyte release out of MSL8	Estimated from conductance (Hamilton et al.[15]) and channel number (Chure et al.[28])
k_{inact}	0.0322 s^{-1}	Rate at which MSL8 inactivates	Fitted to data
Nonlinear elastic wall			
P_c	2.56×10^6 Pa[a,b]	Pressure threshold at which the pollen grain begins to deform	Fitted to data
	2.06×10^6 Pa[c]		
k_p	8.26×10^{-9} Pa^{-1} s^{-1}[a,b]	Rate constant for viscous deformation of the pollen grain	Fitted to data
	7.47×10^{-9} Pa^{-1} s^{-1}[c]		
Constants			
RT	2.48×10^6 J m^{-3} M	Thermodynamic values (gas constant, temperature)	–

[a]Used in the basic model
[b]Used in the inactivation models
[c]Used in the cell wall strengthening model

Variations on the initial model that include membrane unfolding and nonlinear elastic cell wall behavior better reproduce experimental observations

To address the first two discrepancies, we considered possible differences between the pollen grain and other systems that show experimental volume overshoots (*E. coli*[32] and yeast[39]). Freeze-fracture imaging of dry pollen[40] suggests that the desiccated pollen membrane may not be taut but rather has folds of extra material that allow it to expand to some extent without added tension. Simulating this effect involved calculating a strain (ε) value:

$$\varepsilon = \frac{r}{r_0} - 1. \quad \text{(Equation 5)}$$

Once the strain reached a threshold (ε_{min}), it was assumed that all membrane reserves had fully unfolded, and membrane tension started to build:

$$\sigma = K_m(\varepsilon - \varepsilon_{min}) \text{ if } \varepsilon > \varepsilon_{min}. \quad \text{(Equation 6)}$$

Incorporation of membrane unfolding lowered the final simulated membrane tension to physically reasonable values and removed some of the overshoot seen in the WT simulation (Figure 2B). In all models hereafter, we adjusted ε_{min} to keep WT tension below the lytic level.

Nevertheless, the *msl8* simulation in the membrane-unfolding model still showed a stabilized volume rather than the characteristic continued expansion seen in wet lab experiments (Figure 2B). Plant cell walls are structurally complex and mechanically dynamic and therefore are unlikely to behave as a simple, linear elastic material.[41] To see if a different material behavior could better simulate the experimental data, we incorporated nonlinear elasticity into the model by calculating the cell pressure (p):

Please cite this article in press as: Miller et al., *In vitro* experiments and kinetic models of *Arabidopsis* pollen hydration mechanics show that MSL8 is not a simple tension-gated osmoregulator, Current Biology (2022), https://doi.org/10.1016/j.cub.2022.05.033

CellPress

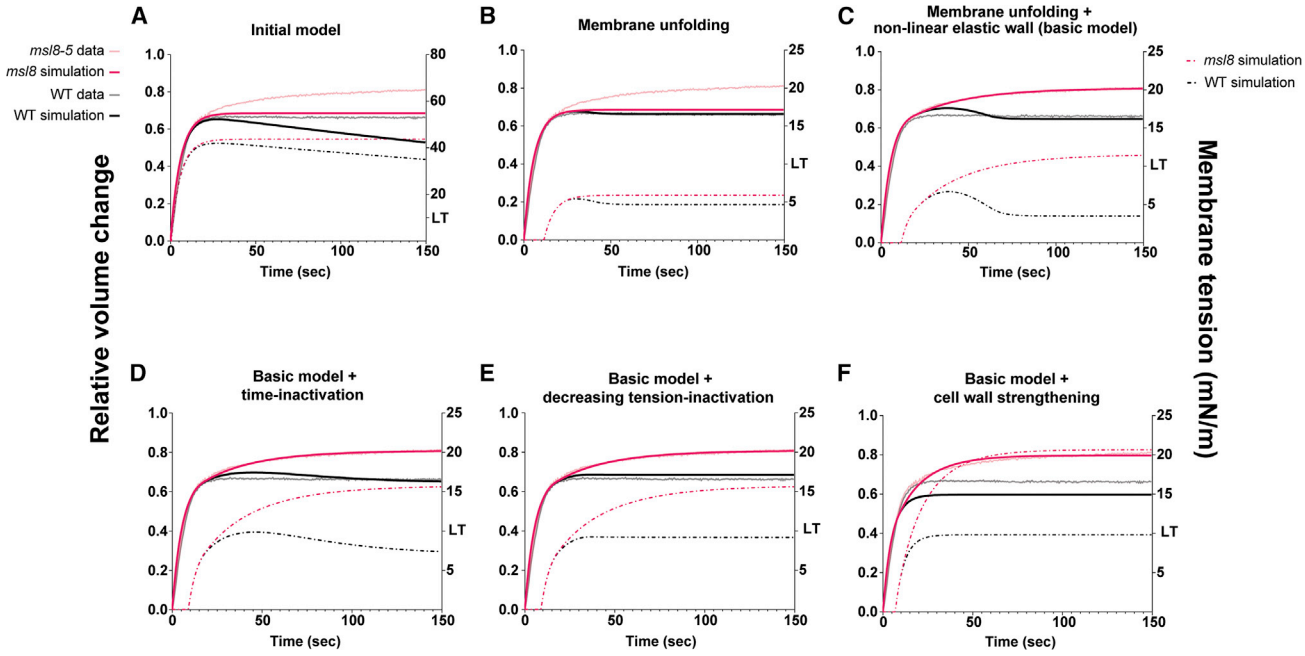

Figure 2. Multiple kinetic models of pollen hydration volume compared with experimental observations

(A) Simulations from the initial model for pollen hydration, which assumes that osmolyte release through the MSL8 channel begins when the tension threshold (σ_{open}) is met, then channel function ceases when the tension decreases past the threshold. There is no osmolyte release in the *msl8* simulation.

(B) Simulations from the membrane-unfolding model, which is the initial model plus the assumption that membrane tension does not increase until the cell reaches a certain amount of strain (ε_{min}).

(C) Simulations from the membrane-unfolding + nonlinear elastic deformation model (referred to hereafter as the "basic model"). Additional deformation of the cell wall occurs when the pressure exceeds a critical threshold (p_c).

(D) The time-inactivation model assumes that ion flux through the MSL8 channel function begins when the tension threshold (σ_{open}) is met, then channel function ceases after a period of time (k_{inact}). Nonlinear elastic deformation of the cell wall is possible in both WT and *msl8* simulations.

(E) The decreasing tension-inactivation model assumes that ion flux through the MSL8 channel begins when the tension threshold (σ_{open}) is met, then ceases as soon as membrane tension begins to decrease. Nonlinear elastic deformation of the cell wall is possible in both WT and *msl8* simulations.

(F) The cell wall strengthening model that assumes MSL8-dependent cell wall strengthening but no osmoregulation. Nonlinear elastic deformation is possible in the *msl8* model but not the WT.

The estimated lytic membrane tension threshold is indicated ("LT" = 10 mN m^{-1}). See also Figure S2.

$$p = 2K\left(\frac{r}{r_0} - 1\right)\Big/ r \qquad \text{(Equation 7)}$$

and setting a critical pressure threshold (p_c). Only after the pressure exceeded this critical pressure would the cell wall undergo a nonlinear deformation (strain softening), determined by a deformation rate constant (k_p):

$$\frac{dr}{dt} = L_p\left[RT(c - c_{ext}) - 2\left(\frac{K}{r}\right)\left(\frac{r}{r_0} - 1\right)\right] + k_p(p - p_c)r \text{ if } p > p_c. \qquad \text{(Equation 8)}$$

We termed this model, which incorporates both membrane unfolding and nonlinear elastic cell wall behavior, the "basic model." The basic model predictions aligned well with experimental observations in that WT pollen grains stabilized in volume while *msl8* pollen continued to expand (a slight overshoot in WT remained; Figure 2C). Membrane tension in the *msl8* simulation did rise above the lytic tension, but we did not consider this to be unrealistic because *msl8* pollen can explode during the hydration process (Figure S1C).[15] We note that the basic model is insensitive to changes in cell wall modulus values between 5 and 5,000 MPa (Figure S2A).

Adding channel inactivation or MSL8-dependent effects on cell wall stiffness produce models that fit experimental data

We next tested the effect of several variations on MSL8 channel behavior on the ability of the model to remove the overshoot and produce a stable volume in WT pollen grains after ~30 s of hydration. Adjusting the threshold gating tension (σ_{open}) of the MSL8 channel or assuming different osmolyte buildup before or during hydration did not produce improved fits (Figure S2B) but three other variations did (Figures 2D and 2F). The first variation, which we call the "time-inactivation model," assumed that channel inactivation occurs spontaneously with a fixed rate. This phenomenon has been suspected to occur with other MS channels, and is a well-documented behavior of MscS.[42] We introduced a closing rate (k_{inact}) for MSL8 that was determined by fitting to the experimental data (Table 1). The closing rate was used to modify the rate at which osmolytes were released:

Please cite this article in press as: Miller et al., *In vitro* experiments and kinetic models of *Arabidopsis* pollen hydration mechanics show that MSL8 is not a simple tension-gated osmoregulator, Current Biology (2022), https://doi.org/10.1016/j.cub.2022.05.033

$$\frac{dk_{flux}}{dt} = -k_{inact}k_{flux} \text{ if } \sigma > \sigma_c. \quad \text{(Equation 9)}$$

Compared with the basic model, the time-inactivation model had improved fit to the experimental data, but it retained a small, temporary volume overshoot in the WT (Figure 2D).

A second model variation, the "decreasing tension-inactivation model," assumed that inactivation occurred as soon as the membrane tension started to decrease (but not necessarily dropping below the closing tension threshold of the channel). MSL10 shows a related behavior in that its threshold tension and open probability are dependent on the rate at which tension is applied to the membrane.[43,44] Incorporating this modification into the basic model only required that k_{flux} be set to zero when the change in membrane tension $(d\sigma/dt)$ becomes less than zero. The decreasing tension-inactivation model variation fit the data well (Figure 2E). The curve shapes for both WT and *msl8* pollen simulations were indistinguishable from the experimental data. However, as in the time-inactivation model, membrane tension in the *msl8* mutant simulation was 1.3–2 times over the estimated lytic tension of a protoplast membrane. Although *msl8* mutant pollen does burst, many grains remain intact (Figure S1C), suggesting that the cell wall helps support the membrane.

We next asked if MSL8 might contribute to pollen survival not directly through the release of osmolytes but indirectly through modulation of cell wall stiffness. MSL8 could either promote stiffening or suppress softening. In the "cell wall strengthening model," we removed all osmotic regulation by MSL8 by setting the k_{flux} value to zero. Instead, we assumed that the presence of MSL8 channels reinforces the cell wall, thus making it more resistant to nonlinear elastic deformation. This is reflected in the model by making the WT cell wall resistant to additional expansion (i.e., omitting the deformation term) while the *msl8* simulation undergoes deformation past the p_c pressure threshold (i.e., retaining the deformation term). Due to the assumption that osmolytes do not leave the pollen grain in either simulation, the c_0 value was fitted to the WT experimental data instead of *msl8* (STAR Methods). Compared with the osmoregulation-based models, this model resulted in poorer accuracy in that the values do not line up with the experimental results, especially around 30 s into hydration (Figure 2F). However, the overall curve shapes were similar to the experimental results in this model. Thus, the experimental behavior of WT and *msl8* pollen grains during the first 150 s of hydration can be reasonably well simulated with a channel that inactivates or one that serves to strengthen the cell wall. We also tested the possibility that MSL8 suppresses the buildup of osmolytes (without effective osmolyte release through the channel) either during development or during the hydration process (Figures S2C–S2E), but neither simulation aligned well with the experimental data.

Hydration in an osmolyte-rich solution restores volume stabilization in *msl8* mutant pollen and in all three model variations

To further probe the role of MSL8 as an osmoregulator during pollen hydration, we tested the robustness of each model to experimental perturbations. We measured the response of WT and *msl8* mutant pollen to hydration in an osmolyte-rich solution, which we predicted would reduce the hypoosmotic shock and thus suppress the requirement for MSL8 to stabilize the pollen volume. We previously found that hydration of *msl8-4* pollen in a PEG 3350 solution instead of water helped restore pollen viability.[15] We replicated that approach here by hydrating the pollen in 20% (w/v) PEG 3350 and recording the first 150 s of hydration. As shown in Figures 3A and S3A, the stabilization of WT pollen volume after 50 s of hydration was unaffected by the addition of PEG to the hydration solution. Although the rapid initial hydration of *msl8-5* pollen was also unaffected, its continued expansion in DI water was suppressed in 20% PEG (Figures 3A and S3B). Linear regression to quantify the slope between 50 and 150 s of hydration indicated that although the slope of the WT volume curve was zero in both water and PEG, the volume curve of *msl8-5* in water had a slope that was significantly nonzero in water ($p < 0.001$) but zero in 20% PEG (Figure 3B).

We next challenged our simulations with hydration in the presence of PEG. To do so, we adjusted the external osmotic concentration, c_{ext}, in the change in radius calculation (Equation 4). To simulate hydration in 20% PEG 3350, we used a c_{ext} of 0.326 Osm.[35] To simulate hydration in water, c_{ext} was set to 0 (as in previous iterations of the model). Simulations were carried out for the two inactivation models and the cell wall strengthening model, and the simulated slopes were calculated (Figures 3C and S3C–S3E). All three models predicted a stabilization of the *msl8* pollen volume in the presence of 20% PEG, consistent with our expectations and with the experimental data shown in Figures 3A and 3B. The difference in final volumes seen in the model (but not in the wet lab data) was not solved by simulating strain stiffening of the cell wall (Figure S3F).

The cell wall strengthening model best simulated the effects of additional desiccation on *msl8* mutant pollen

If, as hypothesized, MSL8 functions as an osmoregulator, increasing cytoplasmic osmolarity could exacerbate the *msl8* mutant phenotype. To test the effect of cytoplasmic osmolarity on pollen hydration, we placed freshly dehiscent pollen in a vacuum chamber overnight for additional dehydration before starting the hydration imaging assay. We found that, for the most part, this treatment had no effect on the initial volume (Figure S4A) or the kinetics of pollen volume changes during hydration (Figure 4A). However, this extra-desiccated pollen had a slightly higher relative volume change after hydration than pollen incubated overnight at ambient conditions. For WT pollen, a slight increase was not statistically significant. However, *msl8-5* pollen swelled significantly more when extra-desiccated (Figure 4B).

To simulate the effect of extra desiccation in the three models, the initial osmotic concentration (c_0) parameter was increased. We found that increasing c_0 by more than 10% resulted in extremely high membrane tension (Figure S4B). Thus, we tested 2%, 5%, and 10% increases in c_0 and examined the predicted final relative volume and membrane tension (Figures 4C–4E and S4C–S4E). In time-inactivation model simulations and, to some degree, the decreasing tension-inactivation model simulations, *msl8* and WT pollen increased both final volume and membrane tension with increasing c_0 (Figures 4C and 4D). However, cell wall strengthening model simulations showed increased swelling and tension in *msl8* pollen with increasing c_0, whereas WT pollen did not change appreciably (Figure 4E). Thus, increasing cytoplasmic osmolarity through extra desiccation

Please cite this article in press as: Miller et al., *In vitro* experiments and kinetic models of *Arabidopsis* pollen hydration mechanics show that MSL8 is not a simple tension-gated osmoregulator, Current Biology (2022), https://doi.org/10.1016/j.cub.2022.05.033

CellPress

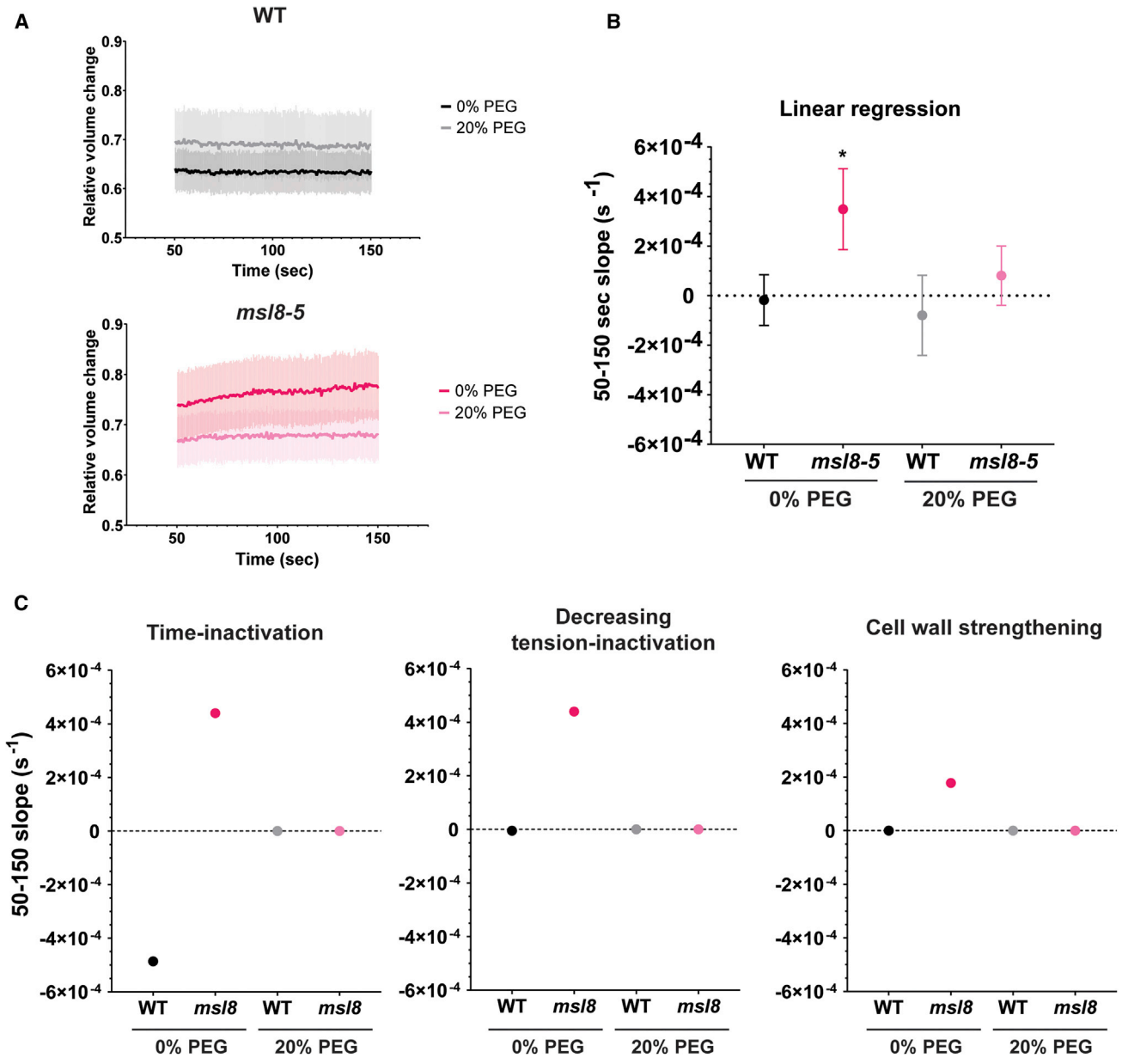

Figure 3. Hydration in an osmolyte-rich solution restores volume stabilization in *msl8* mutant pollen

(A) The stabilization period (between 50 and 150 s after the addition of the hydration solution) of WT (top) and *msl8-5* (bottom) pollen grains hydrated in water (0%) or in 20% (w/v) PEG 3350 (n = 30 pollen grains for each genotype and treatment). Bars are 95% CI. Full-length curves are in Figure S3. There is no significant difference between the final relative volume change of WT in 0% and 20% PEG (Mann-Whitney test; $p = 0.39$), but there is a significant difference between *msl8-5* in 0% and 20% PEG (Mann-Whitney test; $p = 0.042$).

(B) Slopes of the data in (A), estimated via simple linear regression for each genotype and treatment. Asterisks indicate the slope was significantly different from zero ($p < 0.05$), which was determined via F test.

(C) Simulations of hydration in water and 20% PEG via modification of c_{ext}.

See also Figure S3.

exacerbated swelling in *msl8* mutant pollen, but not in the WT, as predicted by our hypothesis that MSL8 functions as an osmoregulator during hydration. However, the fact that the cell wall strengthening model was the best at simulating this effect suggested that cell wall extensibility rather than osmolyte release could be the key difference between WT and *msl8* mutant pollen under these conditions.

Overexpressing MSL8-YFP does not affect pollen volume stabilization, and this was best replicated in the decreasing tension-inactivation and cell wall strengthening models

Next, we examined the effect of increased MSL8 channel number on pollen grain volume during hydration. If MSL8 functions as an osmotic safety valve, we would expect that additional

Please cite this article in press as: Miller et al., *In vitro* experiments and kinetic models of *Arabidopsis* pollen hydration mechanics show that MSL8 is not a simple tension-gated osmoregulator, Current Biology (2022), https://doi.org/10.1016/j.cub.2022.05.033

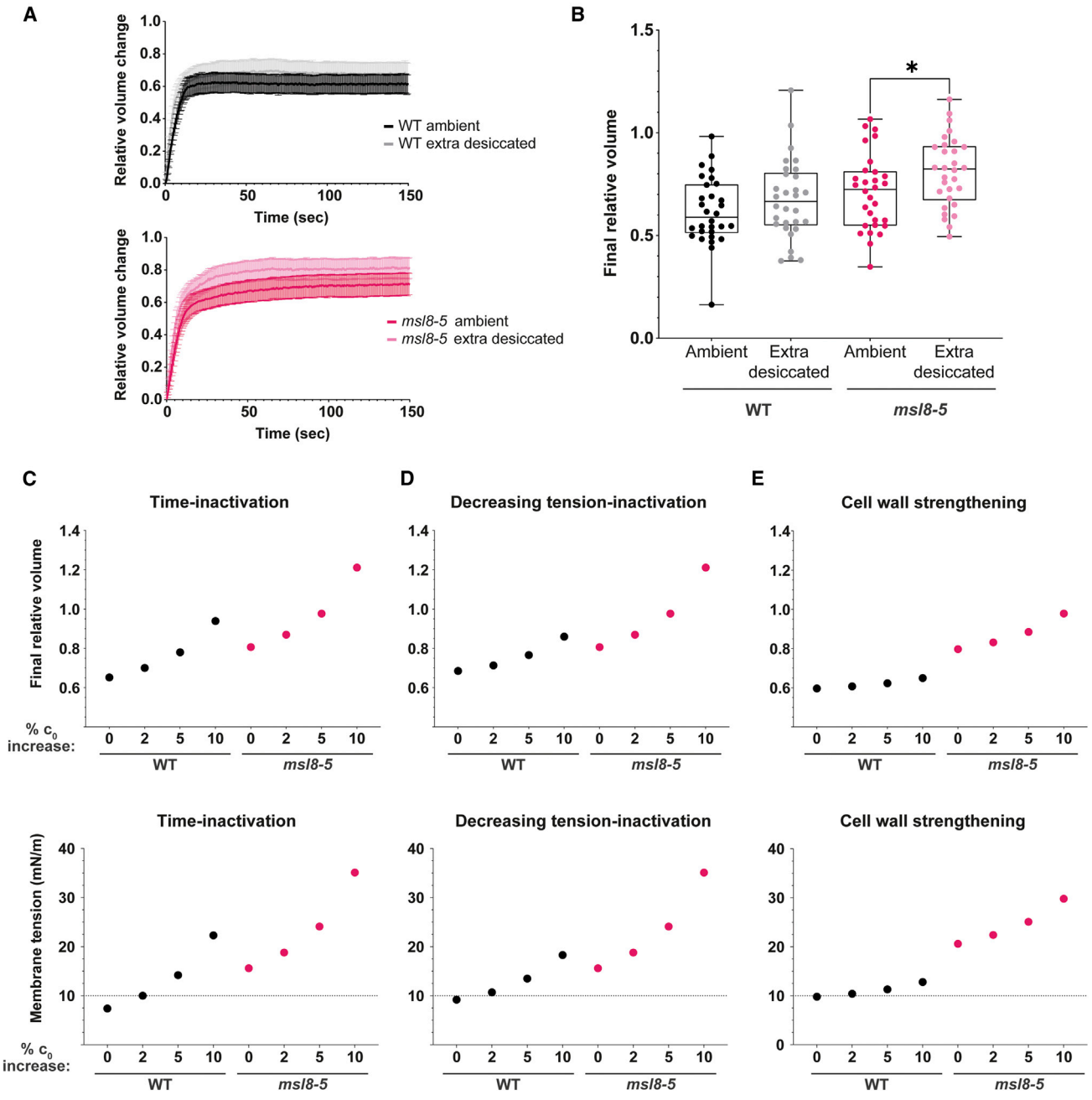

Figure 4. Increasing cytoplasmic osmolarity exacerbates swelling in *msl8* mutant pollen during hydration

(A) Relative size change over time of hydrating WT (top) and *msl8-5* (bottom) pollen grains incubated overnight in either a vacuum chamber or ambient conditions (n = 30 pollen grains per genotype per treatment). Bars are 95% CI.

(B) Final (150 s after hydration) relative volume change for pollen grains in the experiment shown in (A). Mann-Whitney U test performed between the extra-desiccated and ambient treatment for each genotype. Grubbs test for outliers did not identify any outliers. *msl8-5* p value = 0.042. WT p value = 0.22.

(C–E) Final relative volume and membrane tension in simulations after altering c_0 in the indicated kinetic models.

See also Figure S4.

channels would release more osmolytes and result in a lower final volume after pollen hydration. We therefore overexpressed MSL8-YFP via the pollen-specific *LAT52* promoter (*LAT52-$_{pro}$:MSL8-YFP*)[15,45] in the Col-0 background. This construct was previously characterized in the *Ler* background, where *MSL8* transcript levels were up to 12 times higher in MSL8-YFP overexpression lines than in the WT.[15,16] These lines are likely to have increased MSL8 channel conductance, as overexpressed MSL8-YFP protein has normal subcellular localization in hydrated pollen grains,[15,16] and introducing a pore-blocking mutation prevented MSL8-YFP overexpression phenotypes.[16] We identified four heterozygous overexpression lines (OE 13, 17,

Please cite this article in press as: Miller et al., *In vitro* experiments and kinetic models of *Arabidopsis* pollen hydration mechanics show that MSL8 is not a simple tension-gated osmoregulator, Current Biology (2022), https://doi.org/10.1016/j.cub.2022.05.033

CellPress

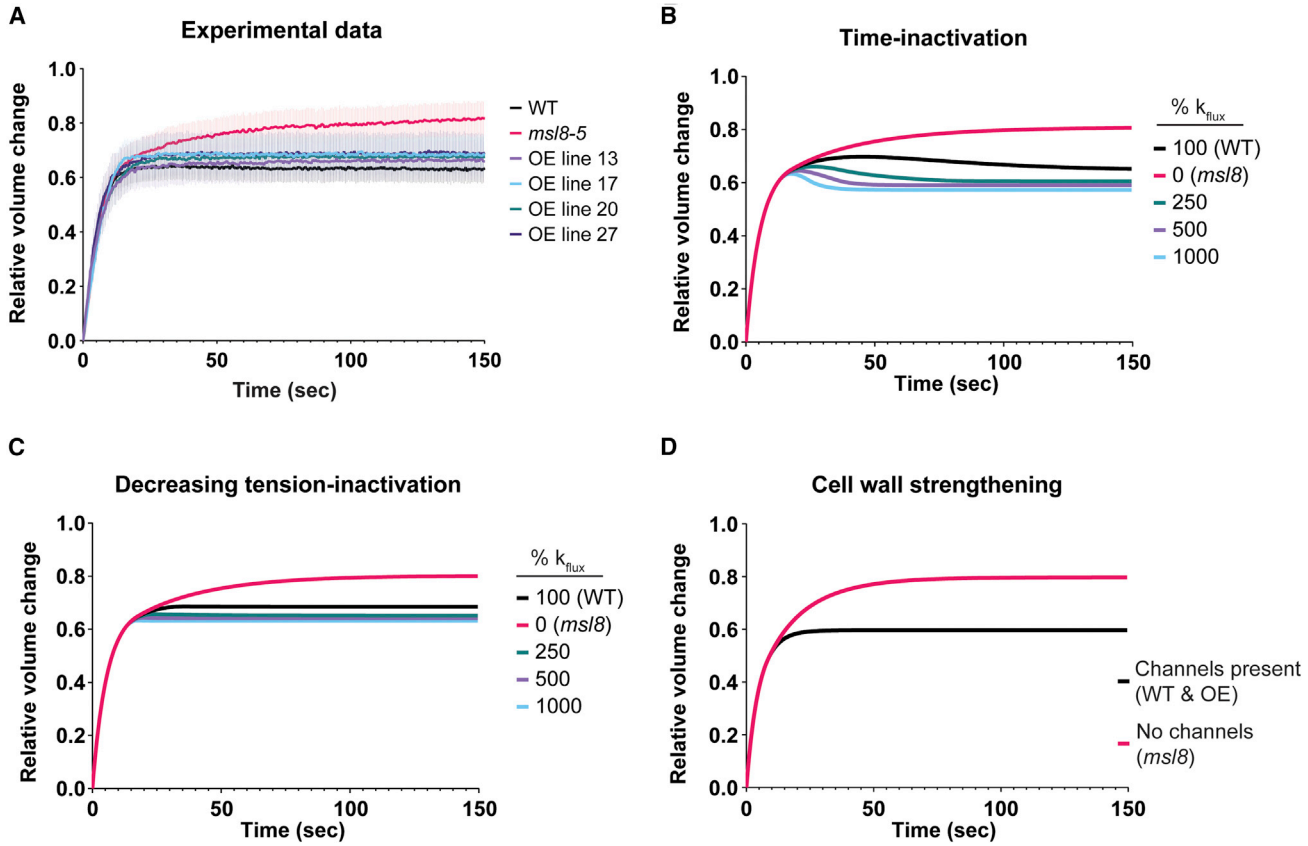

Figure 5. Overexpressing *MSL8-YFP* does not affect volume stabilization during pollen hydration

(A) Relative size change over time of hydrating pollen grains overexpressing (OE) *MSL8-YFP* (n = 30 grains per genotype). Bars are 95% CI.

(B and C) Time-inactivation and decreasing tension-inactivation model results with varying relative values of the k_{flux} parameter.

(D) Cell wall strengthening model results. Note that there is no effective osmolyte release (i.e., no k_{flux} parameter); thus, this result is the same as in Figure 2F. See also Figure S5.

20, and 27) with strong YFP fluorescence in pollen grains (Figure S5A). We were unable to identify homozygous lines, likely due to previously documented effects of MSL8 overexpression on male fertility.[15,16] Although pollen grains overexpressing MSL8-YFP were smaller than WT pollen (Figure S5B), their relative volume change curves were indistinguishable from those of WT pollen (Figure 5A).

To include MSL8 overexpression in the models, effective channel activity was increased by modifying the channel ion flux rate, k_{flux}. We set 0% channel function to be equivalent to *msl8* while 100% channel function was equivalent to WT. Further increases in k_{flux} represented MSL8 overexpression. Both the time-inactivation model and the decreasing tension-inactivation model were relatively insensitive to k_{flux}; hence, channel function could be increased up to 1,000% without resulting in a relative volume change lower than 0.5, which is the lower end of the 95% confidence intervals (Figures 5B and 5C). The time-inactivation model showed an overshoot and recovery when channel function was high, which was not reflected in the experimental data (Figure 5A). However, the decreasing tension-inactivation model fit the experimental data well, with very little effect from increased channel function. The cell wall strengthening model does not have channel function; hence, there was no k_{flux} value to increase and this model therefore matched this experimental result (Figure 5D). To summarize, we found that, unexpectedly, overexpressing MSL8-GFP did not alter the kinetics of swelling in hydration experiments. Furthermore, two of our models (decreasing tension-inactivation and cell wall strengthening) simulated the experimental data well, suggesting that MSL8 does not function as a simple tension-gated osmoregulator.

Pore-blocked MSL8 channels do not prevent overexpansion during pollen hydration

We next tested to see if ion flux through MSL8 was required for volume stabilization. To do this, we used a MSL8 point mutation ($MSL8^{F720L}$) previously shown to abolish ion conductance and fail to protect pollen during hydration.[16] MSL8-GFP or $MSL8^{F720L}$-GFP was expressed from the *MSL8* promoter in the *msl8-5* background using previously described transgenes ($MSL8_{pro}$*:MSL8-GFP* and $MSL8_{pro}$*:*$MSL8^{F720L}$*-GFP*).[16] Three lines were selected for each transgene, and stable, full-length protein expression was confirmed via immunoblot (Figure S6A). Phenotypes were assessed using the initial hydration assay (Figure S6B). As expected, a transgene harboring the genomic version of *MSL8* complemented the *msl8-5* phenotype, as

Please cite this article in press as: Miller et al., *In vitro* experiments and kinetic models of *Arabidopsis* pollen hydration mechanics show that MSL8 is not a simple tension-gated osmoregulator, Current Biology (2022), https://doi.org/10.1016/j.cub.2022.05.033

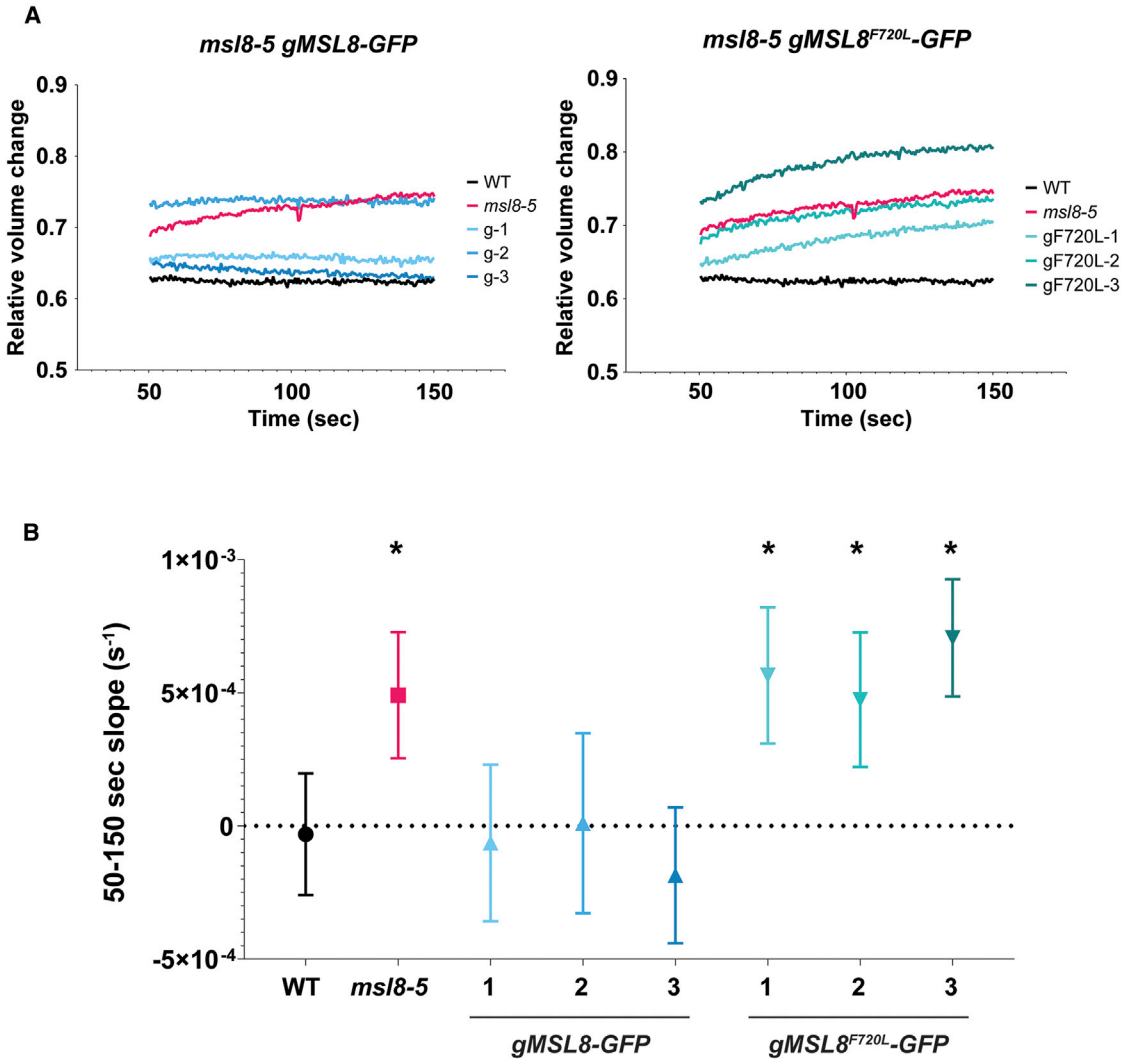

Figure 6. MSL8 channel conductance is required for pollen grain volume stabilization

(A) Experimental hydration results of pollen expressing *gMSL8-GFP* (left) and *gMSL8^{F720L}-GFP* (right) (n = 30 grains for each). Only the relative volume between 50 and 150 s is displayed as this section was used to estimate a slope; full-length curves are shown in Figure S6.

(B) Slopes estimated via simple linear regression for each genotype. Asterisks indicate that the slope was significantly different from zero (marked with a dashed line) which was determined via F test ($p < 0.05$). Bars are 95% CI.

See also Figure S6.

msl8-5 MSL8$_{pro}$:MSL8-GFP pollen stabilized in volume between 50 and 150 s of hydration (Figure 6A). Quantification showed a slope that was not significantly different from zero in all three lines (Figure 6B). However, *msl8-5 MSL8$_{pro}$:MSL8^{F720L}-GFP* pollen continued to expand, similar to *msl8-5* pollen, and showed a nonzero slope between 50 and 150 s (Figures 6A and 6B). Thus, osmolyte conductance through MSL8 is necessary for the volume stabilization seen in WT pollen.

DISCUSSION

Plant cell mechanics is complicated by the presence of a cell wall and multiple atmospheres of turgor pressure. *In vitro* pollen grain hydration represents a relatively simple starting place for modeling plant cell mechanics due to the absence of neighbors, the isotropic nature of expansion, and the involvement of a single MS ion channel, MSL8. Here, we characterized the kinetics of pollen swelling during the first 150 s of pollen hydration under a range of osmotic conditions and MSL8 levels. In addition, we developed and tested several related models of pollen hydration that incorporated different assumptions about cell wall mechanics, membrane mechanics, and MS channel function. Multiple mathematical descriptions of pollen tube tip growth[46,47] and of pollen grain desiccation and swelling[48–50] have been developed but do not directly address the role of MS channels. Here, our primary goal was to test the hypothesis that MSL8 acts as an osmotic safety valve to regulate pollen volume during the hypoosmotic shock of hydration, as is well-established for bacterial MS channels.[29–31] We conclude that our results do not support this hypothesis.

Please cite this article in press as: Miller et al., *In vitro* experiments and kinetic models of *Arabidopsis* pollen hydration mechanics show that MSL8 is not a simple tension-gated osmoregulator, Current Biology (2022), https://doi.org/10.1016/j.cub.2022.05.033

The role of the membrane

It is likely that the desiccated state of the pollen grain affects the function of any membrane-embedded proteins, including MS ion channels. Although there is some discrepancy,[51,52] freeze-fracture electron microscopy studies indicate a continuous membrane around the outside of the pollen protoplast during early hydration.[40,53] However, these membranes show ruffling and may not be under tension.[40,53] Such folds could delay the buildup of membrane tension, changing the kinetics of MS ion channels. Incorporating this possibility into our model made it more accurate by producing a realistic membrane tension and reducing the volume overshoot. Large membrane reserves have been previously documented in animal cells[54–56] and may serve as a mechanism for preventing or delaying the activation of mechanosensitive processes.

Another consideration is membrane renewal via exocytosis. We found that not all *msl8* pollen grains burst (Figure S1C), but our modeling suggested a membrane tension that rises above a lytic threshold (Figures 2C–2F). How is the membrane avoiding rupture? We find it unlikely that additional plasma membrane is being exocytosed during hydration, as (1) it takes over a minute for fluorescent protein to be transported to the tip of an actively growing pollen tube tip,[57] (2) complete plasma membrane renewal is estimated to take between 10 min (in nonexpanding cells) and 3 h (in expanding cells),[58] and (3) the desiccated pollen grain is in a state of metabolic inactivity.[6] Instead, the cell wall may be providing additional support to the membrane. Future studies should seek to further understand the nature of the desiccated pollen grain membrane, its interactions with the cell wall, and its influence on hydration mechanics.

The role of the cell wall

Plant cell wall material is described as "viscoelastoplastic," meaning it behaves as an elastic material until a high enough force is applied, then it exhibits stress relaxation as part of the viscoplastic response.[59] This material property is thought to be the result of many cell wall components interacting and contributing strength and/or flexibility.[5] Indeed, a pollen hydration model that assumed the wall is a simple elastic material did not capture the volume dynamics we observed experimentally, and we were unable to simulate the slow expansion seen in *msl8* pollen (compare red lines in Figures 2A and 2B). By incorporating nonlinear deformation past a pressure threshold (rather than a limiting pressure threshold), we were able to simulate experimental results in the basic model (Figure 2C). Although this did create a small overshoot in the WT simulation , in the model variations , the pressure threshold was never reached, there was no additional deformation of the cell wall and the volume remained stable, aligning with our experimental results (Figures 2D–2F). Additional aspects of cell wall mechanics, such as the hydration of absorbent pectin gels,[12,13,60] should be incorporated into future iterations of the model and may address the discrepancy between this model and experimental results when pollen is hydrated in 20% PEG (Figures 3A and S3C–S3E).

Most pollen cell walls are nonuniform, with large gaps in the exine layer that expose the intine beneath to the environment.[61] Other models have addressed the role of such apertures on desiccation[48,49] and hydration.[50] Božič and Šiber considered the structure of the cell wall as a function of volume (which is a fixed parameter) and developed a model to determine how differences in wall stiffness influence the possibility of bursting in pollen with a single pore-like aperture.[50] *Arabidopsis* pollen has larger, elongated apertures that primarily contribute to expansion latitudinally.[9] After the first 20 s of hydration, *msl8* pollen grains continue to expand equally in both the length and width directions (Figure S1G), suggesting that this phenotype is distinct from aperture unfolding. However, future models should consider the influence of apertures on *Arabidopsis* pollen hydration mechanics and the potential role of cell wall heterogeneity in preventing bursting.

MSL8 does not function as a simple osmotic safety valve during pollen hydration

Our previous characterizations of MSL8's role in maintaining pollen viability led us to hypothesize that it acts as an osmotic safety valve, similar to MscS in *E. coli*.[15,16,24–28,31,32,62] Indeed, a pore-blocked MSL8 variant was unable to rescue the *msl8* phenotype, confirming that ion flux through the channel is necessary in some capacity to prevent over-expansion during pollen hydration (Figure 6). However, our basic model, wherein MSL8 acts as a simple osmotic safety valve, did not fit the experimental data (Figure 2C). We thus added three variations to the basic model: (1) MSL8 inactivates after some time; (2) MSL8 inactivates when the tension starts to decrease; and (3) the key aspect of MSL8 channel function is not osmoregulation, but cell wall stiffening. Below, we discuss these three possibilities in the context of existing literature on MS channel dynamics and cell wall mechanics.

Time inactivation or decreasing tension inactivation of MSL8

Modeling channel inactivation after time passed (time inactivation; Figure 2D) or after tension began to decrease (decreasing tension inactivation; Figure 2E) either partially or fully recapitulated the volume stabilization seen in WT pollen, respectively. Both models successfully predicted the effects of PEG hydration and extra desiccation on *msl8* pollen. The time-inactivation model failed to predict several experimental observations; furthermore, time inactivation has not been observed for MSL8.[15] In fact, MSL1,[63] MSL10,[43] and MSL8[15] all close much more slowly than they open, thereby maintaining an extended open state.

Cell wall strengthening by MSL8

This model successfully predicted the effect of hydration in PEG (Figure 3C) and extra desiccation on both WT and *msl8* pollen (Figure 4E), as well as the hydration phenotype of pollen overexpressing MSL8-YFP (Figure 5D). However, these results beg the question: how would ion flux through MSL8 affect cell wall properties? MSL8 is likely to transport anions,[15] so its activation would depolarize the membrane and both directly and indirectly alter apoplastic anion concentrations and pH. Several components that impact the stiffness of the cell wall in the cell wall, such as cellulose, hemicellulose, and pectin, have complex electrostatic interactions[64] that could be affected by the ionic strength of the apoplast. Moreover, recently reported complex interactions between MSL8 and the cell wall integrity pathway, including modification of callose deposition shortly before and after pollen germination, suggest a role for MSL8 in adaptive

cell wall responses.[17] Future studies of the effect of MSL8 on cell wall composition and strength will be crucial to experimentally test this intriguing model.

Conclusions and future directions

The data presented here reveal that MSL8 stabilizes pollen volume during the initial stages of hydration but not via simple osmoregulation as we originally hypothesized. Rather, it suggests that the MSL8 channel exhibits unusual inactivation behavior or that it affects pollen cell wall properties. This work further highlights the utility of mathematical modeling for testing assumptions in proper physical context while also developing new, testable hypotheses. We demonstrated that our assumption of MSL8 function—which was based on MS channel function in other systems—was not entirely correct. Future computational work should incorporate the ellipsoid shape of the pollen grain, add cell wall heterogeneity like apertures, and eventually address the polarized nature of hydration and expansion that occurs in vivo and during tube germination. Overall, we believe that this model of single plant cell mechanics will be useful as we seek to understand how osmotic regulation and cell wall integrity influence one another.

STAR★METHODS

Detailed methods are provided in the online version of this paper and include the following:

- KEY RESOURCES TABLE
- RESOURCE AVAILABILITY
  - Lead contact
  - Materials availability
  - Data and code availability
- EXPERIMENTAL MODEL AND SUBJECT DETAILS
  - Plant Materials
  - Accession Numbers
- METHOD DETAILS
  - Constructs and plant transformation
  - Expression confirmation via immunoblot
  - Pollen hydration imaging
  - Model parameter calculations and fitting procedures
- QUANTIFICATION AND STATISTICAL ANALYSIS

SUPPLEMENTAL INFORMATION

Supplemental information can be found online at https://doi.org/10.1016/j.cub.2022.05.033.

ACKNOWLEDGMENTS

This work was supported by the NSF Graduate Research Fellowship (DGE-2139839 and DGE-1745038) to K.M., William H. Danforth Fellowship in Plant Sciences to K.M., NSF MCB 1929355 to E.S.H. and A.C., and the NSF Center for Engineering Mechanobiology (NSF grant CMMI 1548571). This work was initiated at a Cell Biology Hackathon supported by NSF grant MCB 1411898 to Wallace Marshall. The graphical abstract was created with BioRender.com.

AUTHOR CONTRIBUTIONS

K.M., A.C., and E.S.H. designed the experiments. K.M., W.S., M.N., A.C., and E.S.H. developed the model. K.M. performed the wet lab experiments and data analysis. K.M., A.C., and E.S.H. wrote the manuscript.

DECLARATION OF INTERESTS

The authors declare no competing interests.

INCLUSION AND DIVERSITY

While citing references scientifically relevant for this work, we also actively worked to promote gender balance in our reference list.

Received: October 18, 2021
Revised: April 12, 2022
Accepted: May 12, 2022
Published: June 3, 2022

REFERENCES

1. Sampathkumar, A. (2020). Mechanical feedback-loop regulation of morphogenesis in plants. Development *147*, dev177964.
2. Braidwood, L., Breuer, C., and Sugimoto, K. (2014). My body is a cage: mechanisms and modulation of plant cell growth. New Phytol *201*, 388–402.
3. Mano, H., and Hasebe, M. (2021). Rapid movements in plants. J. Plant Res. *134*, 3–17.
4. Smithers, E.T., Luo, J., and Dyson, R.J. (2019). Mathematical principles and models of plant growth mechanics: from cell wall dynamics to tissue morphogenesis. J. Exp. Bot. *70*, 3587–3600.
5. Codjoe, J.M., Miller, K., and Haswell, E.S. (2022). Plant cell mechanobiology: greater than the sum of its parts. Plant Cell *34*, 129–145.
6. Pacini, E., and Dolferus, R. (2019). Pollen developmental arrest: maintaining pollen fertility in a world with a changing climate. Front. Plant Sci. *10*, 679.
7. Rozier, F., Riglet, L., Kodera, C., Bayle, V., Durand, E., Schnabel, J., Gaude, T., and Fobis-Loisy, I. (2020). Live-cell imaging of early events following pollen perception in self-incompatible *Arabidopsis thaliana*. J. Exp. Bot. *71*, 2513–2526.
8. Zheng, Y.-Y., Lin, X.-J., Liang, H.-M., Wang, F.-F., and Chen, L.-Y. (2018). The long journey of pollen tube in the pistil. Int. J. Mol. Sci. *19*, 3529.
9. Wang, R., and Dobritsa, A.A. (2018). Exine and aperture patterns on the pollen surface: their formation and roles in plant reproduction. Annu. Plant Rev. Online *1*, 1–40.
10. Moon, S., and Jung, K.-H. (2020). First steps in the successful fertilization of rice and *Arabidopsis*: pollen longevity, adhesion and hydration. Plants (Basel) *9*, E956.
11. Leroux, C., Bouton, S., Kiefer-Meyer, M.-C., Fabrice, T.N., Mareck, A., Guénin, S., Fournet, F., Ringli, C., Pelloux, J., Driouich, A., et al. (2015). PECTIN METHYLESTERASE48 is involved in *Arabidopsis* pollen grain germination. Plant Physiol *167*, 367–380.
12. Vieira, A.M., and Feijó, J.A. (2016). Hydrogel control of water uptake by pectins during in vitro pollen hydration of Eucalyptus globulus. Am. J. Bot. *103*, 437–451.
13. Fan, T.-F., Park, S., Shi, Q., Zhang, X., Liu, Q., Song, Y., Chin, H., Ibrahim, M.S.B., Mokrzecka, N., Yang, Y., et al. (2020). Transformation of hard pollen into soft matter. Nat. Commun. *11*, 1449.
14. Windari, E.A., Ando, M., Mizoguchi, Y., Shimada, H., Ohira, K., Kagaya, Y., Higashiyama, T., Takayama, S., Watanabe, M., and Suwabe, K. (2021). Two aquaporins, SIP1;1 and PIP1;2, mediate water transport for pollen hydration in the *Arabidopsis* pistil. Plant Biotechnol. (Tokyo) *38*, 77–87.
15. Hamilton, E.S., Jensen, G.S., Maksaev, G., Katims, A., Sherp, A.M., and Haswell, E.S. (2015). Mechanosensitive channel MSL8 regulates osmotic forces during pollen hydration and germination. Science *350*, 438–441.
16. Hamilton, E.S., and Haswell, E.S. (2017). The tension-sensitive ion transport activity of MSL8 is critical for its function in pollen hydration and germination. Plant Cell Physiol. *58*, 1222–1237.

17. Wang, Y., Coomey, J., Miller, K., Jensen, G.S., and Haswell, E.S. (2022). Interactions between a mechanosensitive channel and cell wall integrity signaling influence pollen germination in *Arabidopsis thaliana*. J. Exp. Bot. *73*, 1533–1545.
18. Kloda, A., and Martinac, B. (2001). Mechanosensitive channels in Archaea. Cell Biochem. Biophys. *34*, 349–381.
19. Poole, K. (2022). The diverse physiological functions of mechanically activated ion channels in mammals. Annu. Rev. Physiol. *84*, 307–329.
20. Cox, C.D., Bavi, N., and Martinac, B. (2018). Bacterial mechanosensors. Annu. Rev. Physiol. *80*, 71–93.
21. Martinac, B., Buechner, M., Delcour, A.H., Adler, J., and Kung, C. (1987). Pressure-sensitive ion channel in Escherichia coli. Proc. Natl. Acad. Sci. USA *84*, 2297–2301.
22. Sukharev, S.I., Blount, P., Martinac, B., Blattner, F.R., and Kung, C. (1994). A large-conductance mechanosensitive channel in *E. coli* encoded by mscL alone. Nature *368*, 265–268.
23. Sukharev, S. (2002). Purification of the small mechanosensitive channel of *Escherichia coli* (MscS): the subunit structure, conduction, and gating characteristics in liposomes. Biophys. J. *83*, 290–298.
24. Levina, N., Tötemeyer, S., Stokes, N.R., Louis, P., Jones, M.A., and Booth, I.R. (1999). Protection of *Escherichia coli* cells against extreme turgor by activation of MscS and MscL mechanosensitive channels: identification of genes required for MscS activity. EMBO J. *18*, 1730–1737.
25. Boer, M., Anishkin, A., and Sukharev, S. (2011). Adaptive MscS gating in the osmotic permeability response in E. coli: the question of time. Biochemistry *50*, 4087–4096.
26. Bialecka-Fornal, M., Lee, H.J., and Phillips, R. (2015). The rate of osmotic downshock determines the survival probability of bacterial mechanosensitive channel mutants. J. Bacteriol. *197*, 231–237.
27. van den Berg, J., Galbiati, H., Rasmussen, A., Miller, S., and Poolman, B. (2016). On the mobility, membrane location and functionality of mechanosensitive channels in *Escherichia coli*. Sci. Rep. *6*, 32709.
28. Chure, G., Lee, H.J., Rasmussen, A., and Phillips, R. (2018). Connecting the dots between mechanosensitive channel abundance, osmotic shock, and survival at single-cell resolution. J. Bacteriol. *200*. e00460–18.
29. Kung, C., Martinac, B., and Sukharev, S. (2010). Mechanosensitive channels in microbes. Annu. Rev. Microbiol. *64*, 313–329.
30. Booth, I.R., and Blount, P. (2012). The MscS and MscL families of mechanosensitive channels act as microbial emergency release valves. J. Bacteriol. *194*, 4802–4809.
31. Martinac, B., Nikolaev, Y.A., Silvani, G., Bavi, N., Romanov, V., Nakayama, Y., Martinac, A.D., Rohde, P., Bavi, O., and Cox, C.D. (2020). Cell membrane mechanics and mechanosensory transduction (Chapter 3). In Current Topics in Membranes Membrane Biomechanics, I. Levitan, and A. Trache, eds. (Academic Press), pp. 83–141.
32. Buda, R., Liu, Y., Yang, J., Hegde, S., Stevenson, K., Bai, F., and Pilizota, T. (2016). Dynamics of Escherichia coli's passive response to a sudden decrease in external osmolarity. Proc. Natl. Acad. Sci. USA *113*, E5838–E5846.
33. Zhou, X., Zheng, Y., Wang, L., Li, H., Guo, Y., Li, M., Sun, M.-X., and Zhao, P. (2022). SYP72 interacts with the mechanosensitive channel MSL8 to protect pollen from hypoosmotic shock during hydration. Nat. Commun. *13*, 73.
34. Wolfe, J., and Steponkus, P.L. (1983). Mechanical properties of the plasma membrane of isolated plant protoplasts: mechanism of hyperosmotic and extracellular freezing injury. Plant Physiol. *71*, 276–285.
35. Schiller, L.R., Emmett, M., Santa Ana, C.A., and Fordtran, J.S. (1988). Osmotic effects of polyethylene glycol. Gastroenterology *94*, 933–941.
36. Suzuki, T., Masaoka, K., Nishi, M., Nakamura, K., and Ishiguro, S. (2008). Identification of kaonashi mutants showing abnormal pollen exine structure in *Arabidopsis thaliana*. Plant Cell Physiol. *49*, 1465–1477.
37. Nezhad, A.S., Naghavi, M., Packirisamy, M., Bhat, R., and Geitmann, A. (2013). Quantification of the Young's modulus of the primary plant cell wall using Bending-Lab-On-Chip (BLOC). Lab Chip *13*, 2599–2608.
38. Le Roux, A.-L., Quiroga, X., Walani, N., Arroyo, M., and Roca-Cusachs, P. (2019). The plasma membrane as a mechanochemical transducer. Philos. Trans. R. Soc. Lond. B Biol. Sci. *374*, 20180221.
39. Altenburg, T., Goldenbogen, B., Uhlendorf, J., and Klipp, E. (2019). Osmolyte homeostasis controls single-cell growth rate and maximum cell size of *Saccharomyces cerevisiae*. NPJ Syst. Biol. Appl. *5*, 34.
40. Platt-Aloia, K.A., Lord, E.M., DeMason, D.A., and Thomson, W.W. (1986). Freeze-fracture observations on membranes of dry and hydrated pollen from Collomia, Phoenix and Zea. Planta *168*, 291–298.
41. Digiuni, S., Berne-Dedieu, A., Martinez-Torres, C., Szecsi, J., Bendahmane, M., Arneodo, A., and Argoul, F. (2015). Single cell wall nonlinear mechanics revealed by a multiscale analysis of AFM force-indentation curves. Biophys. J. *108*, 2235–2248.
42. Vásquez, V. (2013). MscS inactivation: an exception rather than the rule. An extremophilic MscS reveals diversity within the family. Biophys. J. *104*, 1391–1393.
43. Maksaev, G., and Haswell, E.S. (2012). MscS-Like10 is a stretch-activated ion channel from *Arabidopsis thaliana* with a preference for anions. Proc. Natl. Acad. Sci. USA *109*, 19015–19020.
44. Tran, D., Girault, T., Guichard, M., Thomine, S., Leblanc-Fournier, N., Moulia, B., de Langre, E., Allain, J.-M., and Frachisse, J.-M. (2021). Cellular transduction of mechanical oscillations in plants by the plasma-membrane mechanosensitive channel MSL10. Proc. Natl. Acad. Sci. USA *118*. e1919402118.
45. Twell, D., Yamaguchi, J., and McCormick, S. (1990). Pollen-specific gene expression in transgenic plants: coordinate regulation of two different tomato gene promoters during microsporogenesis. Development *109*, 705–713.
46. Fayant, P., Girlanda, O., Chebli, Y., Aubin, C.-É., Villemure, I., and Geitmann, A. (2010). Finite element model of polar growth in pollen tubes. Plant Cell *22*, 2579–2593.
47. Dumais, J. (2021). Mechanics and hydraulics of pollen tube growth. New Phytol. *232*, 1549–1565.
48. Katifori, E., Alben, S., Cerda, E., Nelson, D.R., and Dumais, J. (2010). Foldable structures and the natural design of pollen grains. Proc. Natl. Acad. Sci. USA *107*, 7635–7639.
49. Božič, A., and Šiber, A. (2020). Mechanical design of apertures and the infolding of pollen grain. Proc. Natl. Acad. Sci. USA *117*, 26600–26607.
50. Božič, A., and Šiber, A. (2022). Mechanics of inactive swelling and bursting of porate pollen grains. Biophys. J. *121*, 782–792.
51. Shivanna, K.R., and Heslop-Harrison, J. (1981). Membrane state and pollen viability. Ann. Bot. *47*, 759–770.
52. Elleman, C.J., and Dickinson, H.G. (1986). Pollen-stigma interactions in Brassica. IV. Structural reorganization in the pollen grains during hydration. J. Cell Sci. *80*, 141–157.
53. Kerhoas, C., Gay, G., and Dumas, C. (1987). A multidisciplinary approach to the study of the plasma membrane of Zea mays pollen during controlled dehydration. Planta *171*, 1–10.
54. Zhang, Y., and Hamill, O.P. (2000). On the discrepancy between whole-cell and membrane patch mechanosensitivity in *Xenopus* oocytes. J. Physiol. *523*, 101–115.
55. Groulx, N., Boudreault, F., Orlov, S.N., and Grygorczyk, R. (2006). Membrane reserves and hypotonic cell swelling. J. Membr. Biol. *214*, 43–56.
56. Gauthier, N.C., Fardin, M.A., Roca-Cusachs, P., and Sheetz, M.P. (2011). Temporary increase in plasma membrane tension coordinates the activation of exocytosis and contraction during cell spreading. Proc. Natl. Acad. Sci. USA *108*, 14467–14472.
57. Luo, N., Yan, A., and Yang, Z. (2016). Measuring exocytosis rate using corrected fluorescence recovery after photoconversion. Traffic *17*, 554–564.
58. Steer, M.W. (1988). Plasma membrane turnover in plant cells. J. Exp. Bot. *39*, 987–996.

59. Fruleux, A., Verger, S., and Boudaoud, A. (2019). Feeling stressed or strained? A biophysical model for cell wall mechanosensing in plants. Front. Plant Sci. *10*, 757.

60. Thompson, D.S., and Islam, A. (2021). Plant cell wall hydration and plant physiology: an exploration of the consequences of direct effects of water deficit on the plant cell wall. Plants (Basel) *10*, 1263.

61. Halbritter, H., Ulrich, S., Grímsson, F., Weber, M., Zetter, R., Hesse, M., Buchner, R., Svojtka, M., and Frosch-Radivo, A. (2018). Illustrated Pollen Terminology (Springer International Publishing).

62. Basu, D., and Haswell, E.S. (2017). Plant mechanosensitive ion channels: an ocean of possibilities. Curr. Opin. Plant Biol. *40*, 43–48.

63. Lee, C.P., Maksaev, G., Jensen, G.S., Murcha, M.W., Wilson, M.E., Fricker, M., Hell, R., Haswell, E.S., Millar, A.H., and Sweetlove, L.J. (2016). MSL1 is a mechanosensitive ion channel that dissipates mitochondrial membrane potential and maintains redox homeostasis in mitochondria during abiotic stress. Plant J. *88*, 809–825.

64. Anderson, C.T., and Kieber, J.J. (2020). Dynamic construction, perception, and remodeling of plant cell walls. Annu. Rev. Plant Biol. *71*, 39–69.

65. Shamsudhin, N., Laeubli, N., Atakan, H.B., Vogler, H., Hu, C., Haeberle, W., Sebastian, A., Grossniklaus, U., and Nelson, B.J. (2016). Massively parallelized pollen tube guidance and mechanical measurements on a lab-on-a-chip platform. PLoS One *11*, e0168138.

66. Vogler, H., Draeger, C., Weber, A., Felekis, D., Eichenberger, C., Routier-Kierzkowska, A.-L., Boisson-Dernier, A., Ringli, C., Nelson, B.J., Smith, R.S., and Grossniklaus, U. (2013). The pollen tube: a soft shell with a hard core. Plant J *73*, 617–627.

67. Edlund, A.F., Zheng, Q., Lowe, N., Kuseryk, S., Ainsworth, K.L., Lyles, R.H., Sibener, S.J., and Preuss, D. (2016). Pollen from *Arabidopsis thaliana* and other Brassicaceae are functionally omniaperturate. Am. J. Bot. *103*, 1006–1019.

68. Qu, Z., and Meredith, J.C. (2018). The atypically high modulus of pollen exine. J. R. Soc. Interface *15*, 20180533.

69. Bidhendi, A.J., and Geitmann, A. (2019). Methods to quantify primary plant cell wall mechanics. J. Exp. Bot. *70*, 3615–3648.

70. Schindelin, J., Arganda-Carreras, I., Frise, E., Kaynig, V., Longair, M., Pietzsch, T., Preibisch, S., Rueden, C., Saalfeld, S., Schmid, B., et al. (2012). Fiji: an open-source platform for biological-image analysis. Nat. Methods *9*, 676–682.

Please cite this article in press as: Miller et al., *In vitro* experiments and kinetic models of *Arabidopsis* pollen hydration mechanics show that MSL8 is not a simple tension-gated osmoregulator, Current Biology (2022), https://doi.org/10.1016/j.cub.2022.05.033

STAR★METHODS

KEY RESOURCES TABLE

REAGENT or RESOURCE	SOURCE	IDENTIFIER
Antibodies		
Living Colors A.v. Monoclonal Antibody (JL-8); anti-GFP	Takara Bio Clontech	Cat # 632380; RRID: AB_10013427
Goat Anti-Mouse IgG Antibody, HRP conjugate	Millipore-Sigma	Cat # 12-349; RRID: AB_390192
Monoclonal Mouse Anti-α-Tubulin antibody	Millipore-Sigma	Cat # T5168-100UL; RRID: AB_477579
Bacterial and virus strains		
Agrobacterium tumefaciens GV3101	N/A	N/A
Chemicals, peptides, and recombinant proteins		
Murashige and Skoog Basal Salt Mixture	PhytoTechnology laboratories	Cat# M404
Agar, Micropropagation Grade	PhytoTechnology laboratories	Cat# A296
PEG 3350	Millipore Sigma	Cat#: P4338
Phosphinothricin	GoldBio	Cat#: P-165
Critical commercial assays		
SuperSignal West Femto Detection Kit	Thermo Fisher Scientific	Cat# 34094
SuperSignal West Dura Detection Kit	Thermo Fisher Scientific	Cat# 34075
Deposited data		
MATLAB code for hydration simulations	This paper	https://doi.org/10.5281/zenodo.6537314
Experimental models: Organisms/strains		
Arabidopsis thaliana Col-0 wild-type	Arabidopsis Biological Resource Center	N/A
msl8-5	[21]	Transgenic Col-0
msl8-8	[21]	Transgenic Col-0
msl7-1 msl8-6	[21]	Transgenic Col-0
msl7-1 msl8-7	[21]	Transgenic Col-0
$LAT52_{pro}$:*MSL8-YFP* (Lines # 13, 17, 20, 27)	This paper	Transgenic Col-0
msl8-5 $MSL8_{pro}$:*MSL8-GFP* (Lines # 1, 2, 3)	This paper	Transgenic *msl8-5*
msl8-5 $MSL8_{pro}$:$MSL8^{F720L}$-*GFP* (Lines # 1, 2, 3)	This paper	Transgenic *msl8-5*
Recombinant DNA		
$LAT52_{pro}$:*MSL8-YFP*	[19]	N/A
$MSL8_{pro}$:*MSL8-GFP*	[20]	N/A
$MSL8_{pro}$:$MSL8^{F720L}$-*GFP*	[20]	N/A
Software and algorithms		
MATLAB v9.4 (R2018a)	Mathworks	https://www.mathworks.com/
Olympus Fluoview FV3000 imaging software	Olympus Life Science	https://www.olympus-lifescience.com
Fiji-ImageJ	[65]	https://fiji.sc/
Prism v9.1	GraphPad	https://www.graphpad.com/
Adobe Illustrator v27.0.3	Adobe Systems Incorporated	https://www.adobe.com/products/illustrator.html
Other		
Immun-Blot PVDF membrane	Bio-Rad	Cat# 162-0255
Glass bottom microwell dish (35 mm petri dish, 14 mm microwell)	MatTek	Cat# P35G-1.5-14-C
Olympus FV3000 confocal laser scanning microscope	Olympus Life Science	https://www.olympus-lifescience.com

Please cite this article in press as: Miller et al., *In vitro* experiments and kinetic models of *Arabidopsis* pollen hydration mechanics show that MSL8 is not a simple tension-gated osmoregulator, Current Biology (2022), https://doi.org/10.1016/j.cub.2022.05.033

RESOURCE AVAILABILITY

Lead contact

Further information and requests for resources and reagents should be directed to and will be fulfilled by the lead contact, Elizabeth S. Haswell (ehaswell@wustl.edu).

Materials availability

All materials generated in this study have been donated to the Arabidopsis Biological Resource Center.

Data and code availability

- All data reported in this paper will be shared by the lead contact upon request.
- The MATLAB code associated with this paper has been deposited at GitHub and is publicly available as of the date of publication. The DOI is listed in the key resources table.
- Any additional information required to reanalyze the data reported in this paper is available from the lead contact upon request.

EXPERIMENTAL MODEL AND SUBJECT DETAILS

Plant Materials

Arabidopsis thaliana plants of the Columbia-0 ecotype were used in all experiments. *The msl8-5, msl8-8, msl7-1msl8-6* and *msl7-1msl8-7* mutant lines were previously generated via CRISPR–Cas9 gene editing in WT or the *msl7-1* T-DNA mutant backgrounds.[17] Seed was surface-sterilized using vapor-phase chlorine (100 mL NaClO + 4 mL HCl) for 6 h before being placed on Petri dishes containing 1/2X Murashige and Skoog (MS) medium, 0.8% (w/v) agar, pH 5.7. For transgene selection, 10 mg/mL phosphinothricin was added to the MS media. The plates were incubated for two days at 4°C then transferred to a 24-h light chamber (Conviron CMP6010) with 120 m^{-C} s^{-s} photons at 21°C and 50% relative humidity for 5-6 days. Seedlings were then transferred to soil and grown under 150 m^{-1} s^{-s} photons light intensity in a 16/8-h light/dark chamber (Conviron MTPC96FLEX) at 21°C.

Accession Numbers

The accession numbers for the genes studied here are: At2g17010 (*MSL8*) and At2g17000 (*MSL7*).

METHOD DETAILS

Constructs and plant transformation

To create pollen-specific MSL8-YFP overexpression lines, *LAT52$_{pro}$:MSL8-YFP*[15] was introduced into Col-0 plants using *Agrobacterium tumefaciens* GV3101 strain-mediated transformation via floral dip. Transformants were selected via spraying with a 100 mg/mL phosphinothricin solution at the seedling stage. Expression was confirmed through fluorescence imaging of pollen grains (488 nm excitation, 500-540 nm range detected) (Figure S5).

To create lines expressing MSL8 and MSL8^{F720L} at endogenous levels, *MSL8$_{pro}$:MSL8-GFP* or *MSL8$_{pro}$:MSL8^{F720L}-GFP*[16] were introduced into *msl8-5* plants using *Agrobacterium tumefaciens* GV3101 strain-mediated transformation via floral dip. Transformants were selected via spraying with a 100 mg/mL phosphinothricin solution at the seedling stage.

Expression confirmation via immunoblot

We isolated pollen from plants expressing *MSL8-GFP* from the *MSL8* promoter via centrifugation of ~60-80 flowers in 1 mL of water. The flowers and water were removed before exposing the pollen pellet to two freeze-thaw cycles in liquid nitrogen. The pollen was then resuspended in 90 μL of 2X sample buffer (0.1 M Tris-HCl, 4% (v/v) SDS, 20% (v/v) Glycerol, 0.2% (v/v) bromophenol blue, and 2% (v/v) β-mercaptoethanol). 20 μL of each sample was loaded and the proteins were resolved using 10% (w/v) SDS-PAGE gel followed by transfer to a polyvinylidene difluoride membrane at 100 mA for 12 h. After blocking in 5% (w/v) milk TBS-T, membranes were incubated in anti-GFP (1:5000 dilution) antibodies followed by a 2 h incubation in secondary goat anti-mouse-HRP (1:10,000 dilution). Detection was performed using the SuperSignal West Femto Detection Kit. Afterward, the blot was stripped and re-probed using the same protocol with anti-tubulin (1:20,000 dilution) antibodies and the SuperSignal West Dura Detection Kit.

Pollen hydration imaging

Both time lapse and fluorescence imaging were performed on an Olympus FV3000 confocal laser scanning microscope using a 20X objective. For time lapse imaging, dry pollen was placed onto a glass bottom microwell dish by gently tapping 5-8 freshly opened flowers onto the glass. In some experiments, dishes were immediately used for imaging; in others, dishes were placed into a vacuum chamber for a 12 h desiccation treatment or incubated on the benchtop for ambient treatment. Recording began before water was added, and images were taken every 0.55 seconds over the course of hydration with either deionized water or 20% (w/v) PEG 3350.

Please cite this article in press as: Miller et al., *In vitro* experiments and kinetic models of *Arabidopsis* pollen hydration mechanics show that MSL8 is not a simple tension-gated osmoregulator, Current Biology (2022), https://doi.org/10.1016/j.cub.2022.05.033

Model parameter calculations and fitting procedures

As mentioned above, parameter values were obtained from the literature where possible. We took several points into account when calculating a cell wall stiffness value. Reported values for the Young's modulus of pollen cell walls vary by several orders of magnitude (20-400 MPa for pollen tubes,[37,65,66] 0.17 MPa for pollen grain intine,[67] and 11.9-16000 MPa for exine/sporopollenin[67,68]), probably due to different measurement and analysis techniques.[69] Due to the heterogeneity of the pollen grain wall, the stiffness averaged over the entire Arabidopsis grain is likely to be lower than those reported for exine/sporopollenin. Thus, we chose a value from the upper range of what is reported for pollen tubes (350 MPa), and a wall thickness representative of the intine, to calculate cell wall stiffness (Table 1). The basic model is insensitive to cell wall modulus values between 5-5000 MPa (Figure S2A).

All model code was run in MATLAB Version 9.4 (R2018a). To fit c_0, the value was solved for from the steady state equation:

$$RT \times c_0 \times r_0^3/r^3 = 2 \times K(r - r_0)/r \times r_0$$

For the basic and inactivation models, the initial radius (radius = $\sqrt[3]{3 \times Volume/4\pi}$) and inflection point radius taken from the *msl8-5* data were used to account for loss of osmolytes due to channel function in the WT. For the cell wall strengthening model, the initial and final radius taken from the WT data were used.

After determining the c_0 value, the L_p value was fitted to the data by solving:

$$\left.\frac{dr}{dt}\right|_{initial} = L_p \times RT \times c_0$$

The initial (dr/dt) was determined from the relevant data set by averaging the change in radius every two seconds over the first twenty seconds, then taking the exponential fit (*msl8-5* initial $(dr/dt) = 0.38$; WT initial $(dr/dt) = 0.45$). For other parameter values fitted to the data (see Table 1), goodnessOfFit() with Mean Squared Error cost function was used for iterative searching of the minimized error.

QUANTIFICATION AND STATISTICAL ANALYSIS

Image analysis for pollen hydration involved thresholding followed by particle analysis in FIJI.[70] Only pollen grains that were not touching other grains/debris and did not visibly lyse were included in the analysis. Three biological replicates (N=10 each; total N=30) were used in every experiment. Statistical tests and graphing were performed using GraphPad Prism Version 9.1 for Windows. Significant differences were determined assuming significance at $p \leq 0.05$. The specific statistical test used in each experiment are in the figure legends. Figures were arranged using Adobe Illustrator Version 27.0.3 for Windows.